

A method to analyze the flyability of airplane trajectories with specified engine power

Gilles Labonté^{*1}, Vincent Roberge² and Mohammed Tarbouchi²

¹Department of Mathematics and Computer Science, Royal Military College of Canada,
Kingston, Ontario, Canada

²Department of Electrical Engineering and Computer Engineering, Royal Military College of Canada,
Kingston, Ontario, Canada

(Received September 12, 2023, Revised November 19, 2023, Accepted December 14, 2023)

Abstract. This article introduces a formalism for the analysis of airplane trajectories on which the motion is determined by specifying the power of the engines. It explains a procedure to solve the equations of motion to obtain the value of the relevant flight parameters. It then enumerates the constraints that the dynamical abilities of the airplane impose on the amount of fuel used, the speed, the load factor, the lift coefficient, the positivity and upper boundedness of the power available. Examples of analysis are provided to illustrate the method proposed, with rectilinear and circular trajectories. Two very different types of airplanes are used in the examples: a Silver Fox-like small UAV and a common Cessna 182 Skylane.

Keywords: airplane equation of motion; airplane trajectory; automatic trajectory planning; circular trajectory; power control; rectilinear trajectory

1. Introduction

Our purpose in this work is to contribute to the automation of trajectory planning for fixed-wing airplanes, which is an essential step in rendering unmanned aerial vehicles (UAVs) autonomous. The vehicles considered here are fixed-wing propeller driven airplanes. General trajectory planning involves two steps. Firstly, a path is constructed as a continuous curve in 3D space that has a continuous tangent, which corresponds to the direction of the velocity being continuous. Secondly, a speed is assigned to the vehicle at each point of this path. There are absolute constraints imposed by the nature of the terrain and the dynamical abilities of the vehicle. There is also usually a requirement to optimize certain parameters for the benefit of the mission. Quite a number of optimization approaches have been proposed in this context; see, for example, Poudel *et al.* (2023), Ait Saadi *et al.* (2022) for up-to-date reviews.

For the construction of the paths, Frazzoli *et al.* (2005) have proposed an efficient technique that is the most often used one today. It consists in concatenating elementary path segments, called motion primitives. The primitive segments most usually considered are rectilinear, circular and helical. This approach simplifies appreciably the calculations in that the behavior of the airplane

*Corresponding author, Emeritus Professor, E-mail: gilles.labonte@rmc.ca

on the motion primitives can be analyzed once and for all, and it then suffices to adjust the connections between primitives to construct a path. A variation of this approach that is often used consists in determining waypoints, building a skeleton trajectory made up of connected rectilinear segments that link these points, and then smoothing out the connections so that the path tangent is continuous.

In the present article, we assume that we are given a path that has already been constructed, by whatever means. Our main contribution in this work is the presentation of an approach for efficiently determining the speeds that are allowed on the provided path. It does so by relating the proposed power settings to the values of the basic variables such as the speeds, the lift coefficient, the load factor and the amount of fuel required. It also indicates how to deal with the constraints imposed by the dynamical abilities of the airplane. The aeronautics formalism we use is essentially that found in classical textbooks such as those of Anderson (2000), Stengel (2004). However, we have incorporated in the equations of motion a rarely included term that corresponds to the change in mass due to fuel consumption. We decompose them in the Frenet-Serret coordinates and arrange them in a form that straightforwardly allows to generate their solution with a Runge-Kutta method, when given a power profile. This work is of primordial importance in that the method presented tells if a proposed trajectory is flyable by the airplane, while also providing all the information required for the optimization of the trajectory.

We believe this work to constitute an original contribution; we found few articles that are close to this subject. It will be very helpful for studies such as Gramajo and Shankar (2017) who pose similar questions for UAVs, used in search and coverage missions, and analyze some of the dynamical constraints. Our work has also more general relevance in that it proposes a fundamental tool for the analysis of the motion of any fixed-wing propeller airplane. As such, it could serve for the developers of high-performance UAVs, by complementing analyses such as those of Varsha and Somashekar (2018).

We give examples of our approach to trajectory analysis for rectilinear and circular paths. These types of path segments are important because they are the motion primitives used in one of the main construction methods for complete paths. Our examples involve two very different airplanes: a Silver Fox-like small UAV that has a fixed pitch propeller and a Cessna 182 Skylane that has a constant speed propeller. They differ considerably in size and also in propeller type. Their properties are listed in our Appendix B. The relevant nomenclature can be found in our Appendix A. The equations of motion that we use take into account the change in weight of the airplane as fuel is burned, which is rarely done in other articles, as explained in Labonté (2012), and the influence of the altitude on the dynamical performances of the airplane. At the level of this study, we neglect the effects of the curvature and the rotation of the earth as do Anderson and Stengel.

1.2 Organisation of the article

This article starts with a presentation of the equation of motion for the center of mass of a fixed-wing airplane moving on an arbitrary trajectory. It decomposes this equation in its longitudinal and transversal components. It then sums up the constraints on the flight parameters that are required by the dynamical abilities of the airplane. It then describes the differential equations to be solved when the trajectory of the airplane is specified by the engine power along its path. It explains how to solve these equations with the Runge-Kutta method of order 4. Three examples, each, for the two airplanes considered, are provided to illustrate the proposed trajectory

flyability analysis with its determination of the important flight parameters. The first two are for rectilinear trajectories, one at power off and the other one at full power. The third one is an inclined circular trajectory with power that varies as an arctangent along the path. These examples are solved for the amount of fuel used, the speed, the load factor and the lift required to fly the trajectory. It is demonstrated that all the required constraints are satisfied, for the flight parameters used on these trajectories.

2. The airplane equations of motion

The motion of airplanes can be described by the six degrees of freedom equations for the motion of an object in three dimensions, which are

$$\mathbf{F} = m \frac{d\mathbf{V}}{dt} + m \boldsymbol{\omega} \times \mathbf{V} \quad \text{and} \quad \mathbf{G} = \frac{d\mathbf{H}}{dt} + \boldsymbol{\omega} \times \mathbf{H}$$

in which \mathbf{F} is the force acting on the center of mass of the body, \mathbf{G} is the applied moments or torques around the x, y, z axes, \mathbf{V} is its velocity, the components of $\boldsymbol{\omega}$ are the rotation rates or angular velocities about the three axes x, y, z and \mathbf{H} is its angular momentum.

Cowley and Levy, in Section 15 of their book (1920) underline the fact that a rigorous treatment of curved trajectories is extremely complicated because of the imperfectly known influences of the differences in aerodynamic forces along the wings, due to their non-symmetric role in the motion. They then mention that “any increase of drag due to the angular velocity of the aircraft and the deflections of the control surfaces can be neglected in comparison with the dominant lift-dependent drag”. In his Chapter XVII on “Nonuniform Flight”, Von Mises (1945) he discusses vertical loops and banked horizontal turns. He points out that in curved trajectories, “the air reactions must supply, in addition to the centripetal force ..., a rolling, a pitching, and a yawing moment...” After some calculations, for the banked turn, he comments that, “the moments required for maintaining the steady rotation are unimportant under normal conditions”, Mair and Birdsall in Chapter 8 of their book (1992) make the same comment.

Correspondingly, in the present study, we also assume that, on the trajectories considered, the motion of rotation of the airplane about its center of mass does not affect appreciably the motion of its center of mass. We thus consider only the equation of motion for the center of mass of the airplane, and neglect the terms that correspond to the rotation rate in the first equation. Thus, the material we present should be thought of as a preliminary study of airplane performance. We project a further study in which these terms will be taken into account.

Furthermore, as is often done, we considered that the angle of attack is small enough that calculations can be done as if the thrust, which is actually along the airplane’s body, can be considered to be in the direction of motion. We also do not take into account the perturbations of the atmosphere.

Fundamental to the description of the airplane motion is the shaft brake power P of the engine, described in Chapter 9 of Anderson (2000). Because of their internal combustion nature, the engine produce power that varies with the altitude as the air density varies. This variation is according to the equation

$$P(h) = P(0) \frac{\rho_{\infty}(h)}{\rho_s} \tag{1}$$

in which $\rho_\infty(h)$ is the density of the undisturbed air in front of the airplane at altitude h , ρ_s and $P(0)$ are respectively the value of ρ_∞ and P at sea level. The power produced by the engines is transferred to the propellers that let the power P_A be available to move the airplane, with

$$P_A = \eta P \quad (2)$$

The parameter η is the efficiency of the propeller, which varies with the speed of the airplane (see Appendix B). The power made available P_A must be at least equal to the power required P_R for the airplane motion, which is determined by the equations of motion. For fixed pitch propellers, there is a speed at which η would change sign, going from positive to negative. Although a negative propeller efficiency could be desirable to slow down the airplane when it descends, it is not recommended to let this happens. Indeed, the propeller would then drive the engine and may thus damage it; see the Commercial Aviation Safety Team document (2011). We shall therefore not allow speeds larger than that value.

The rate of fuel burning is described by the equation

$$\frac{dW}{dt} = -cP \quad (3)$$

in which W is the total weight of the airplane, c is the specific fuel consumption. The equations of motion contain the thrust T_R required for the motion to be possible. Clearly, the power available must correspond to this thrust. Chapter 5 of Stengel (2004) explains how the thrust is related to the power, for propeller driven airplanes. The power produced by the propeller P_A moves the air with a thrust T_A across the propeller such that

$$P_A = T_A (V_\infty + DV_i)$$

where V_∞ is the airplane speed and DV_i is the speed increase of the air across the propeller disk. Clearly, even when the airplane is not moving, there would be power required to turn the propellers. The power $T_A V_\infty$ is thus the *useful power* that can propel the airplane, and $T_A DV_i$ is the *induced power* that accelerates the flow of air downstream. The propulsive efficiency η_I is then defined as

$$\eta_I = \frac{V_\infty}{V_\infty + DV_i} \quad \text{so that} \quad \text{useful power} = \eta_I P_A$$

and the thrust can be related to the power available, the airspeed and air density as

$$P_A = T_A \left[\frac{V_\infty}{2} + \sqrt{\left(\frac{V_\infty}{2}\right)^2 + \frac{T_A}{2\rho_\infty A}} \right] \quad (4)$$

where $A = \pi Rad^2$ is the area traced by the propeller of radius Rad when it rotates. When the speed V_∞ is null, the static thrust is

$$T_A = \sqrt[3]{2\rho_\infty A P_A^2}$$

From Eq. (4) there follows that the thrust T_A is related to the power available P_A through a cubic equation, the solution of which is

$$T_A(h, V_\infty, P_A) = P_A^{1/2} (\rho_\infty A)^{1/3} \left\{ \left[P_A^{1/2} - \sqrt{P_A + \frac{8\rho_\infty A V_\infty^3}{27}} \right]^{1/3} + \left[P_A^{1/2} + \sqrt{P_A + \frac{8\rho_\infty A V_\infty^3}{27}} \right]^{1/3} \right\} \quad (5)$$

In Labonté (2012), it was shown how to take into account the change in the mass M of the airplane as fuel is burned. Newton's equation of motion then becomes

$$M \frac{d\mathbf{v}}{dt} - (AFR) \left[\frac{dM}{dt} \right] \mathbf{v} = \mathbf{F}. \quad (6)$$

In this equation, \mathbf{v} is the airplane velocity, (AFR) is the air to fuel ratio in the combustion process, which is about 14.7 for gasoline or diesel (Kamm 2002), and \mathbf{F} is the total force acting on the center of mass of the airplane. \mathbf{F} has four components: the thrust \mathbf{T}_R produced by the engines, the lift produced by the airfoil and the airplane body, the drag due to air resistance and the force of gravity. The unit vector \mathbf{T} is defined as being in the direction of the motion of the center of mass of the airplane. It is therefore tangent to the path and we shall consider that the thrust acts along its direction so that

$$\mathbf{T}_R = T_R \mathbf{T}, \quad (7)$$

The lift \mathbf{L} is

$$\mathbf{L} = L \mathbf{U}_L \text{ with } L = \frac{1}{2} \rho_\infty S C_L V_\infty^2, \quad (8)$$

and where \mathbf{U}_L is the unit vector in the direction of the lift. Assuming that the airplane is bilaterally symmetric, we denote as \mathbf{w} the unit vector along the straight line from its left to its right wing tips. Then $\mathbf{U}_L = \mathbf{w} \times \mathbf{T}$; it is therefore always perpendicular to the direction of the motion that is the same as that of the relative wind. L is generally positive but can also be negative when the lift coefficient C_L is negative, which is possible with certain wing profiles. The drag is

$$\mathbf{D} = -D \mathbf{T} \text{ with } D = \frac{1}{2} \rho_\infty S C_D V_\infty^2 \quad (9)$$

where D is always positive, and the force of gravity is

$$\mathbf{W} = -Mg \mathbf{k}, \quad (10)$$

in which g is the gravitational constant and \mathbf{k} is the unit vector in the positive direction of the earth z -axis.

2.1 Decomposition of Newton's equation

With the values of the force \mathbf{F} given in Eqs. (7) to (10), Newton's Eq. (6) becomes

$$M \left[\frac{dV_\infty}{dt} \mathbf{T} + \frac{V_\infty^2}{R} \mathbf{N} \right] - (AFR) \frac{dM}{dt} V_\infty \mathbf{T} = T_R \mathbf{T} + L \mathbf{U}_L - D \mathbf{T} - Mg \mathbf{k} \quad (11)$$

where \mathbf{T} and \mathbf{N} are respectively the Frenet-Serret unit tangent and unit normal vectors. The projection of Eq. (11) along the vector \mathbf{T} yields the following equation for the longitudinal motion

$$M \frac{dV_\infty}{dt} - (AFR) \frac{dM}{dt} V_\infty = T_R - D - Mg(\mathbf{k} \cdot \mathbf{T}). \quad (12)$$

There are two components of Eq. (11) that are perpendicular to \mathbf{T} : one in the direction of the normal \mathbf{N} and one in the direction of the binormal \mathbf{B} . Its component along \mathbf{N} is

$$L (\mathbf{U}_L \cdot \mathbf{N}) = W A_c \quad \text{in which} \quad A_c = \frac{\kappa V_\infty^2}{g} + (\mathbf{k} \cdot \mathbf{N}) \quad (13)$$

is the centripetal acceleration. It can be negative, for an example, when the airplane is flying right-side-up in the upper part of an inclined circular path. Upon projecting Eq. (11) in the direction of \mathbf{B} , there results

$$L(\mathbf{U}_L \cdot \mathbf{B}) = W(\mathbf{k} \cdot \mathbf{B}). \quad (14)$$

Given Eqs. (13) and (14) and the fact that \mathbf{U}_L has only components along \mathbf{N} and \mathbf{B} , there follows that

$$\mathbf{U}_L = \frac{W}{L} [A_c \mathbf{N} + (\mathbf{k} \cdot \mathbf{B}) \mathbf{B}]. \quad (15)$$

Thus

$$L = Wn, \quad (16)$$

with

$$n = e \sqrt{A_c^2 + (\mathbf{k} \cdot \mathbf{B})^2} \quad (17)$$

in which $e = \pm 1$ is the sign of the lift L , that is, of the lift coefficient C_L . The ramp angle or climb angle $\bar{\theta}$ is

$$\sin(\bar{\theta}) = \mathbf{k} \cdot \mathbf{T}. \quad (18)$$

The angle of roll $\bar{\phi}$ is the angle that the lift makes with the position it would hold if the airplane was moving horizontally at trim condition. In this case, the lift would lie in the vertical plane that contains the longitudinal axis of symmetry of the airplane that passes through its center of mass. This plane is defined as containing the unit vectors \mathbf{T} and \mathbf{k} . The angle of roll $\bar{\phi}$ is therefore

$$\sin(\bar{\phi}) = \mathbf{U}_L \cdot (\mathbf{k} \times \mathbf{T})$$

Upon substituting in this equation, the value of \mathbf{U}_L given in Eq. (15) there results

$$\sin(\bar{\phi}) = \frac{\kappa V_\infty^2}{gn} (\mathbf{k} \cdot \mathbf{B}) \quad (19)$$

3. The absolute physical constraints

There are constraints that ensure the integrity of the structure of the airplane and some that result from the configuration of its airframe and the power of its engines. These are:

- The load factor n is bounded below by n_{\min} and above by n_{\max} , in which the bounds are constants that are respectively negative and positive, with $n_{\max} > 1$ and $n_{\min} \leq -1$. For curved paths, the bound on the load factor imply a lower limit for the turning radius.
- The lift coefficient is bounded below by $C_{L\min}$ et above by $C_{L\max}$. $C_{L\max}$ is always positive and $C_{L\min}$ is usually also positive but it can be negative for certain airfoil profiles. For curved paths, there will be a lower limit on the radius resulting from this bound on the lift coefficient.
- The speed V_∞ is bounded below by the stall speed: V_{stall} at which the lift is not sufficient to sustain the airplane motion. It is bounded above by the value V_{NE} (the suffix NE stands for “Never Exceed”) that is determined by the airplane constructor. For airplanes with a fixed pitch

propeller, there is another upper bound on the speed that corresponds to the requirement that the efficiency of the propeller does not become negative (see Appendix B). It is not recommended to let this happen because then the propeller drives the engine, instead of the other way around, thus causing a negative torque. High levels of negative torque result in high drag and potential engine damage.

- The power available to move the airplane is bounded above according to the capacity of its engines.
- There is also obviously a constraint on the fuel that is available.

4. Trajectories with prescribed power

We consider the situation in which the motion of the airplane is determined by specifying the power provided by the engine(s) P_P along the path. Without loss of generality, we suppose that its value is given by a continuous function P_{fn} of the distance s traveled along the path, as $P_{fn}(s)$ for $s=0$ to s_f =the length of the path. If the power is prescribed only at certain points along the path, a continuous function P_{fn} can then be defined as that of a cubic spline passing through these points. Alternatively, the user may consider that the power maintains the same value given at one position until the next position at which a new value is given.

In this problem, there are three differential equations to solve. The first one is Eq. (2), in which $P=P_{fn}(s)$. The second one is Eq. (12) that describes the longitudinal component of the Newton equation of motion. Upon substituting in it the value of dM/dt , given by Eq. (2), and the value of $T_R=P_R/V_\infty$ and that of the drag force D given as:

$$D = \frac{1}{2} \rho_\infty S C_D V_\infty^2 .$$

Upon replacing L by its value given in Eq. (16), there results the following expression for C_L

$$C_L = \frac{2 W n}{\rho_\infty S V_\infty^2} \tag{20}$$

Correspondingly, the drag D can be written as

$$D = D(h, V_\infty, W) = \frac{1}{2} \rho_\infty S C_{D0} V_\infty^2 + \frac{2W^2 n^2}{\pi e A R \rho_\infty S V_\infty^2} \tag{21}$$

Thus, Eq. (12) becomes the following differential equation for V_∞

$$\frac{dV_\infty}{dt} = \frac{1}{M} \left\{ T_R - \frac{(AFR)c}{g} V_\infty P - D(h, V_\infty, W, n) \right\} - g(\mathbf{k} \cdot \mathbf{T}). \tag{22}$$

Note that using the Runge-Kutta 4 method to solve this equation, requires to dispose of the values of the altitude h and of the projections $\mathbf{k} \cdot \mathbf{T}$, $\mathbf{k} \cdot \mathbf{N}$ and $\mathbf{k} \cdot \mathbf{B}$ that depend on the path. Therefore, these values depend on the value of s , the distance traveled from the start of the trajectory. This value is in turn obtained by solving the following equation

$$\frac{ds}{dt} = V_\infty \tag{23}$$

4.1 Runge-Kutta solution

The system of three equations Eqs. (3), (22), (23) can be written as

$$\frac{d\mathbf{U}}{dt} = \mathbf{F}(t, \mathbf{U}) \quad (24)$$

in which $\mathbf{U}=[W, V_\infty, s]^T$ and the vector valued function \mathbf{F} has the following three components

$$F_1 = -cP(s) \quad (25)$$

$$F_2 = \text{Right Hand Side of Eq. (22)}. \quad (26)$$

$$F_3 = V_\infty \quad (27)$$

In order to solve Eq. (24) with the R-K 4 method, it is necessary to dispose of a small time step dt to iterate the value of the desired parameters. We note that, before solving the equations, there is no way to determine a value of dt so that an integral number of steps of this length will make the solution for s arrive exactly at s_f . The procedure we have adopted consists in selecting some dt , solving the equations, and stopping the R-K 4 calculation at the first step N where $s_N \geq s_f$. If the equality holds, then there is nothing more to do. If s has overpassed s_f , then the last time step length is modified so that, with this last step, s terminates at s_f . We did this by constructing a cubic spline s_{spline} from the sequence of the last five distances $\{s_n\}$ and using it to interpolate and determine the instant t_f at which $s_{spline}(t_f) = s_f$. The last time step that will make the solution arrive exactly at s_f is then set to be of length $t_f - t_{N-1}$.

Once a correct time sequence has been obtained, it is possible to obtain the final values of W and V_∞ , either by representing them as cubic splines in their own right, or by doing the last R-K step with the length of the last time step.

As discussed in Lotkin (1951), the approximation error in a sequence of N steps of the R-K method, for the differential equation

$$\frac{dy}{dt} = \mathbf{F}(t, \mathbf{y}) \quad \text{with the initial condition } y(t_0) = y_0.$$

can be estimated without knowing the exact solution. For time steps of equal length dt , such an estimate is obtained as follows. Let $y_{a1} = y_N$ be the approximate value of y constructed by a sequence of N steps of size dt that ends at time t_N , and $y_{a2} = y_{2N}$ the approximate value obtained with $2N$ steps of size $dt/2$. Then the truncation error $E_1 = \|y(t_N) - y_{a1}\|$, where $y(t_N)$ is the exact value of the solution at time t_N , is of the order of

$$E_1 \approx \frac{16}{15} \|y_{a1} - y_{a2}\|. \quad (28)$$

5. Examples of flyability analysis with prescribed power

We now demonstrate how to use the procedure explained above, by examining the flyability of trajectories for the Silver Fox like UAV and the Cessna 182 Skylane on the following trajectories:

5.1 Rectilinear trajectory at power off

5.2 Rectilinear trajectory at maximum power

5.3 Circular trajectory at altitude varying power

The first two trajectories have been examined from a different point of view in Labonté (2020), where the parameters have been determined to obtain optimal glide and optimal climb. These examples are reviewed here as an illustration of our feasibility analysis method. An example of a circular trajectory with minimal power requirement has been considered in Labonté (2017). The example considered here is different than that one. Not only it provides an illustration of our feasibility analysis method, but it presents also a never before considered way of varying the power on a circular trajectory.

The computation times reported for each example are correspond to our own implementation of the R-K 4 algorithm with the software Matlab, run on a portable Omen laptop from HP with Intel Core i7-10750H CPU@2.60 GHz. They are the average of 10 runs of the same calculation of the solution together with the verification of all the constraints.

5.1 Rectilinear trajectory at power off

On a rectilinear path, the unit tangent vector \mathbf{T} is constant and makes an angle θ with a horizontal plane. Since θ lies in the interval $[-\pi/2, \pi/2]$, $\cos(\theta)$ is always non-negative and lies in the interval $[0, 1]$. This vector \mathbf{T} can be written as

$$\mathbf{T} = [\cos(\theta) \cos(\phi), \cos(\theta) \sin(\phi), \sin(\theta)] \quad (29)$$

The position of the center of mass of the airplane $\mathbf{x}(s)$ is then

$$\mathbf{x}(s) = \mathbf{x}(0) + s\mathbf{T} \quad (30)$$

in which s is the distance traveled from the starting point at $\mathbf{x}(0)$. The curvature κ is null so that the radius of curvature R is infinite. By convention, we select the unit normal vector \mathbf{N} to be horizontal, with

$$\mathbf{N} = [-\sin(\phi), \cos(\phi), 0]. \quad (31)$$

The unit binormal vector \mathbf{B} is then

$$\mathbf{B} = \mathbf{T} \times \mathbf{N} = [-\sin(\theta)\cos(\phi), -\sin(\theta)\sin(\phi), \cos(\theta)] \quad (32)$$

We note that only the scalar products of \mathbf{k} with the Frenet-Serret unit vectors appear in the equation of motion: these are

$$\mathbf{k} \cdot \mathbf{T} = \sin(\theta) \quad \mathbf{k} \cdot \mathbf{N} = 0 \quad \mathbf{k} \cdot \mathbf{B} = \cos(\theta).$$

At power off, the function F_2 in Eq. (21) becomes simply

$$\mathbf{F}_2 = -g \left[\frac{D(h, V_\infty, W)}{W} + \sin(\theta) \right]. \quad (33)$$

5.1.1 Silver Fox-like UAV

In all our examples with the Silver Fox-like UAV, we consider that it starts empty, except for a full tank of fuel that is 19.1 N of gasoline of assumed density of 0.743 kg/l.

In the present example, it starts at the altitude of 1,800 m, which is about half way to its service ceiling, at the initial speed of $V_\infty(0) = 20$ m/s, on a path inclined at -5° with the horizontal. We took

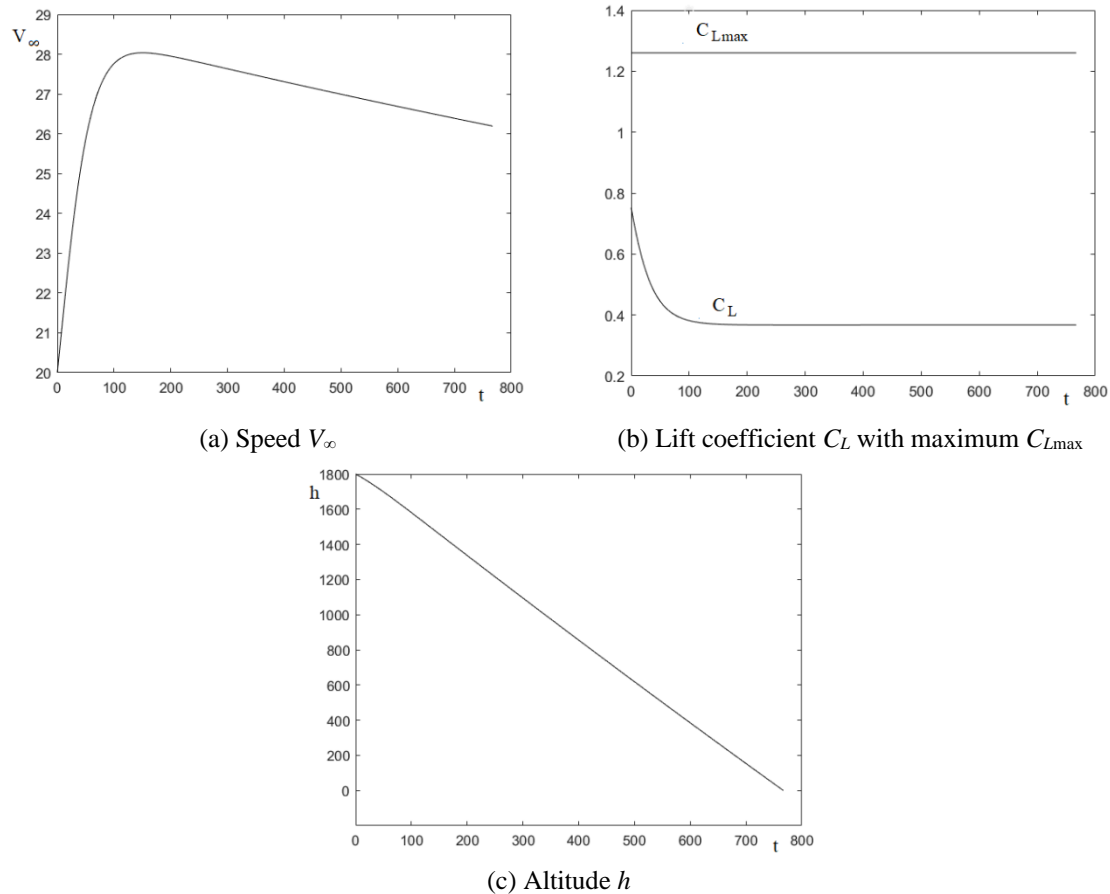


Fig. 1 Flyable rectilinear trajectory with $\theta = -5^\circ/V_\infty(0) = 20$ m/s at power off

a R-K 4 time step $dt = 0.4$ s. The UAV then reached sea level at $t = 12$ min 47 s. The length of the path traveled is 20,652.7 m. Fig. 1 shows how the speed V_∞ , the lift coefficient C_L and the altitude h vary with time along the trajectory. One can see that the speed remains well below its upper bound of 56.4 m/s; the lift coefficient also remains below its bound. The graph in Fig. 1(c) for the altitude shows that its variation is close to linear.

The estimates of the truncation errors, according to Eq. (28), are less than 10^{-12} for all the variables calculated. The R-K 4 solutions are then essentially exact. The average computation time for 10 runs is 0.93 s.

5.1.2 Cessna 182 Skylane

In all our examples with the Cessna Skylane, we consider that it starts empty, except for a full tank of fuel that is 1737 N of 91-octane gasoline of assumed density of 0.743 kg/l.

In the present example, it starts at the altitude of 2,700 m, which is about half way to its service ceiling, at the initial speed of $V_\infty(0) = 40$ m/s, on a path inclined at -5° with the horizontal. We took a R-K 4 time step $dt = 0.4$ s. The Cessna then reached sea level at $t = 11$ min 11 s. The length of the path traveled is 30,979.0 m. Fig. 1 shows how the speed, the lift coefficient and the altitude vary

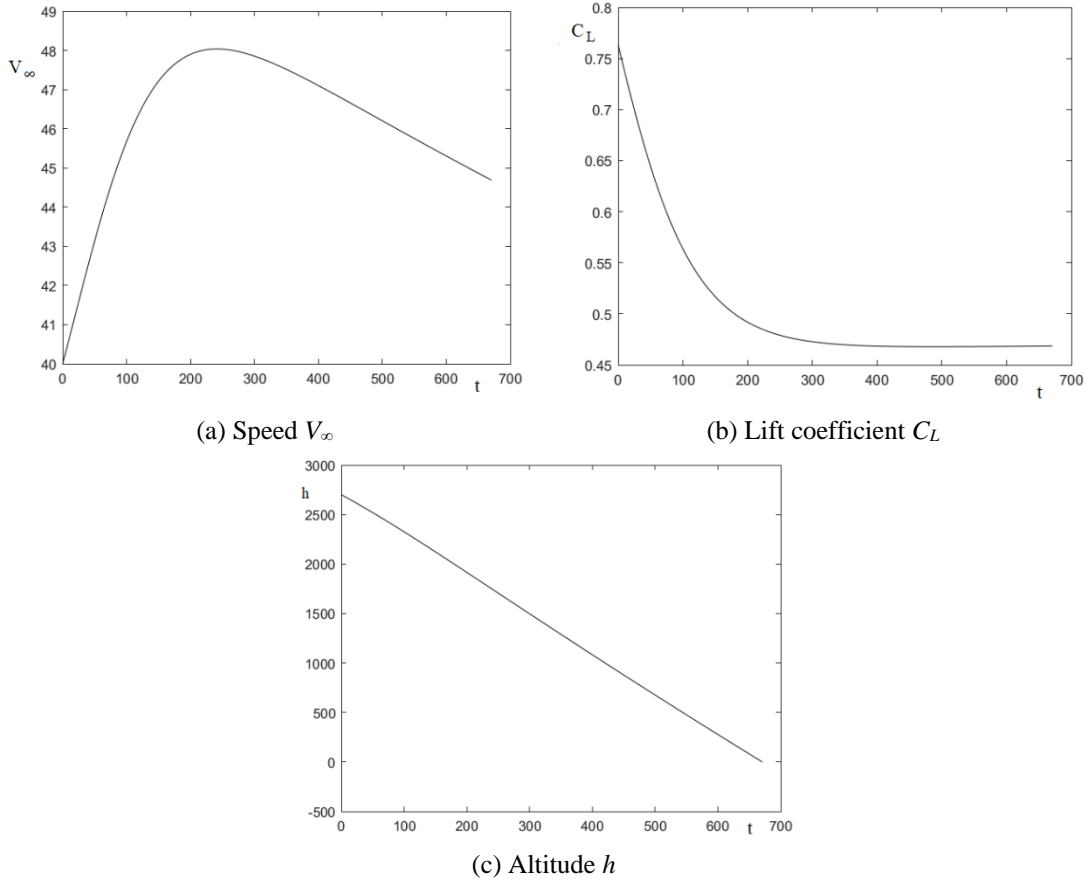


Fig. 2 Flyable rectilinear trajectory with $\theta = -5^\circ / V_\infty(0) = 40$ m/s at power off

with time along the trajectory. The speed remains well below its upper bound of 56.4 m/s; as well as the lift coefficient that has an upper bound of 2.1. Again, as Fig. 2(c) shows, the altitude is close to being linear in time.

The estimates of the truncation errors, according to Eq. (28), are less than 10^{-12} for all the variables calculated. The R-K 4 solutions are then essentially exact. The average computation time for 10 runs is 0.81 s.

5.2 Rectilinear trajectory at full power

Consider that the power produced by the engines is at its maximum value so that

$$P(h) = P_{\max} \frac{\rho_\infty(h)}{\rho_s} \tag{34}$$

in which P_{\max} is the maximum power that the engines can produce at sea level, ρ_s is the air density at sea level and h is the altitude. We note that all the equations of Section 5, except for Eq. (33) are also valid for this path.

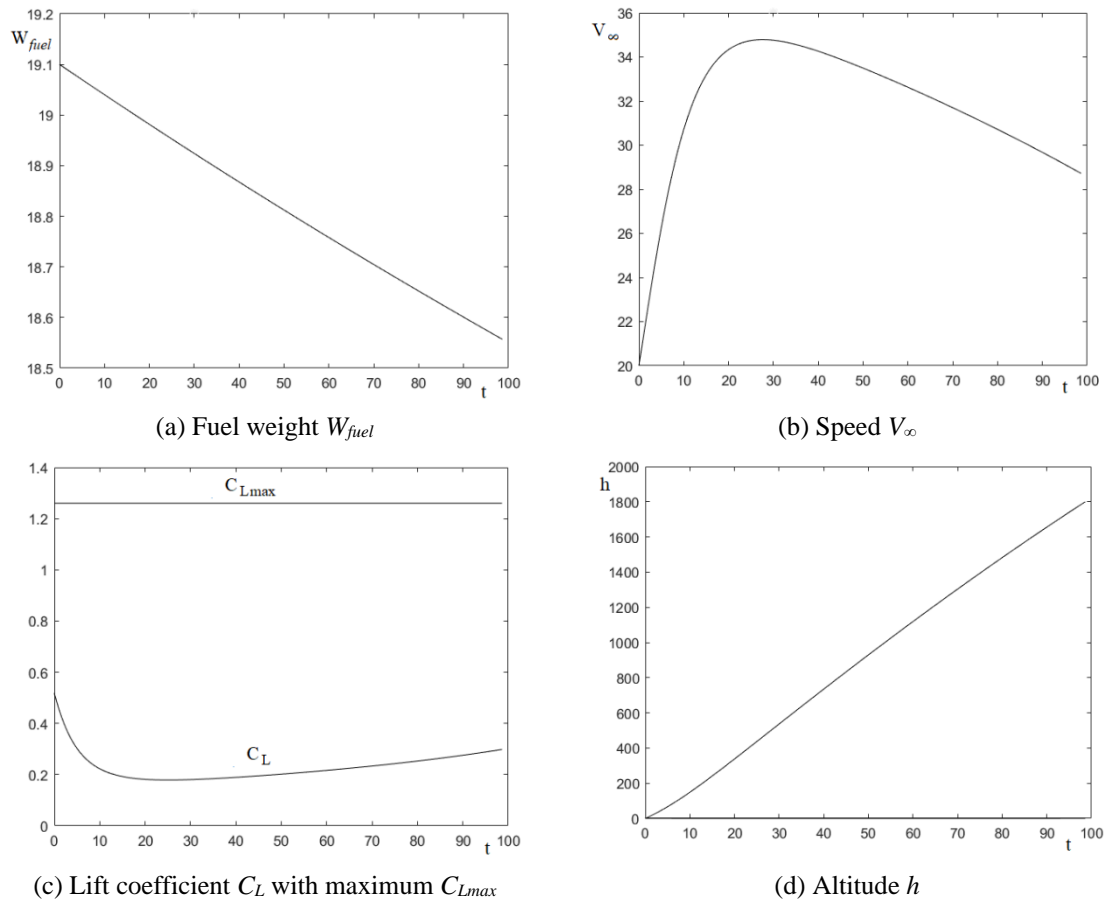


Fig. 3 Flyable rectilinear trajectory with $\theta=35^\circ$ / $V_{\infty}(0)=20$ m/s at full power

5.2.1 Silver Fox-like UAV

When a Silver Fox-like UAV starts at sea level and flies up to 1,800 m, with the initial speed of $V_{\infty}(0)=20$ m/s, on a rectilinear path that is inclined at 35° with the horizontal, it will reach its final altitude at $t=1$ min 39 s. The length of the path traveled is 3,138.2 m. The flight requires 0.543 N of fuel that is about 74.5 ml. Fig. 3 shows how some of the flight parameters vary with time. It is noticeable that the weight of fuel decreases essentially linearly.

Our R-K 4 calculations have been done with $dt=0.2$ s. The estimates of the truncation errors, according to Eq. (28), are

- for the amount of fuel used: less than 1.3×10^{-4} N
- for the speed: less than 5.8×10^{-3} m/s
- for the lift coefficient: less than 3.1×10^{-4}

The R-K 4 method can then be considered to yield, for all practical purposes, exact solutions. The average computation time for 10 runs is 0.24 s.

5.2.2 Cessna 182 Skylane

When a Cessna Skylane starts at sea level and flies up to 2,700 m, with the initial speed of

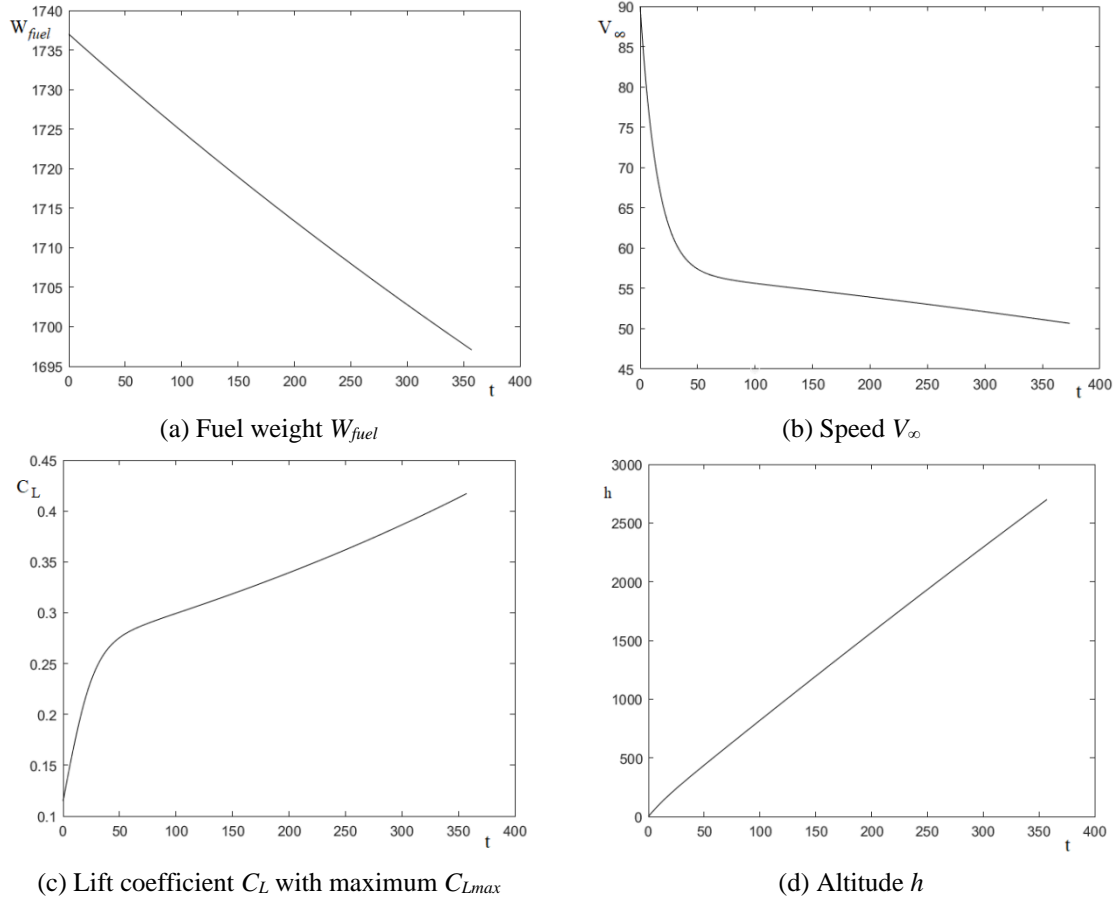


Fig. 4 Flyable rectilinear trajectory with $\theta=55^\circ/V_{\infty}(0)=12$ m/s at full power

$V_{\infty}(0)=90$ m/s, on a rectilinear path that is inclined at 7.5° with the horizontal, it will reach its final altitude at $t=5$ min 57 s. The length of the path traveled is 20,685.5 m. The flight requires 41.73 N of fuel that is about 5.7 l. Fig. 4 shows how some of the flight parameters vary with time. It is noticeable that the weight of fuel decreases close to linearly. The lift coefficient C_L remains well below its maximum value of 2.1.

Our R-K 4 calculations have been done with $dt=0.4$ s. The estimates of the truncation errors, according to Eq. (28), are

- for the amount of fuel used: less than 1.6×10^{-3} N
- for the speed: less than 2.4×10^{-3} m/s
- for the lift coefficient: less than 3.8×10^{-5}

The R-K 4 method can then be considered to yield, for all practical purposes, exact solutions. The average computation time for 10 runs is 0.44 s.

5.3 Circular trajectory at arctangent varying power

Consider a circular path of radius R that is inclined at an angle θ with the horizontal plane.

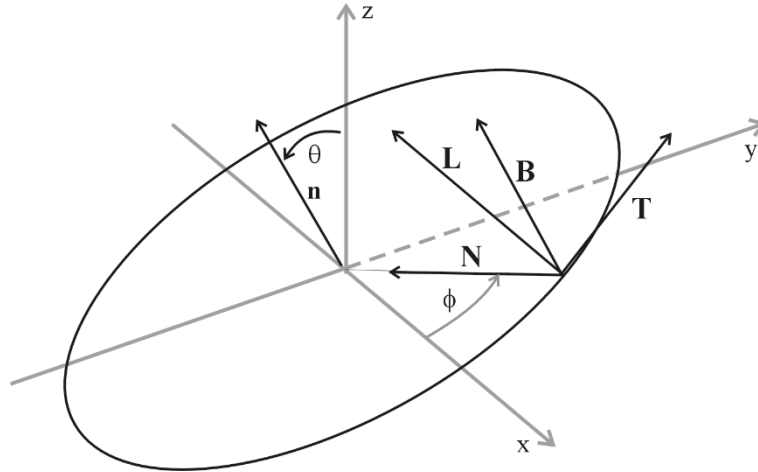


Fig. 5 Frenet-Serret unit vectors T , N , B and lift vector L on the circular trajectory

Without loss of generality in the present discussion, we select the axes so that this circular path is inclined about the x -axis, as shown in Fig. 5.

This circular path is readily described with the help of two orthogonal unit vectors in the plane in which it resides, such as

$$\mathbf{i}=[1, 0, 0] \text{ and } \mathbf{u}=[0, \cos(\theta), \sin(\theta)]. \quad (35)$$

The unit normal vector to this plane is

$$\mathbf{n}=[0, -\sin(\theta), \cos(\theta)].$$

The points on the path can be represented by

$$\mathbf{x}(\phi)=\mathbf{C}+R [\mathbf{i} \cos(\phi) + \mathbf{u} \sin(\phi)] \text{ for } \phi=0 \text{ to } 2\pi. \quad (36)$$

where \mathbf{C} is the position of the center of the circle and the angle ϕ on the path starts on the positive x -axis. The unit tangent vector is

$$\mathbf{T}=[-\sin(\phi), \cos(\theta)\cos(\phi), \sin(\theta)\cos(\phi)] \quad (37)$$

$\kappa=1/R$ and

$$\mathbf{N}=[\cos(\phi), \cos(\theta)\sin(\phi), 0] \quad (38)$$

thus, \mathbf{N} is parallel, but in the opposite direction, to the radius vector. The binormal vector \mathbf{B} is

$$\mathbf{B}=\mathbf{T} \times \mathbf{N}=[0, -\sin(\theta), \cos(\theta)]=\mathbf{n}. \quad (39)$$

The scalar products that enter in the equation of motion are

$$\mathbf{k} \cdot \mathbf{T}=\sin(\theta) \cos(\phi) \quad \mathbf{k} \cdot \mathbf{N}=-\sin(\theta) \sin(\phi) \quad \mathbf{k} \cdot \mathbf{B}=\cos(\theta).$$

According to Eqs. (13) and (17),

$$A_c = \frac{V_\infty^2}{gR} - \sin(\theta) \sin(\phi) \quad (40)$$

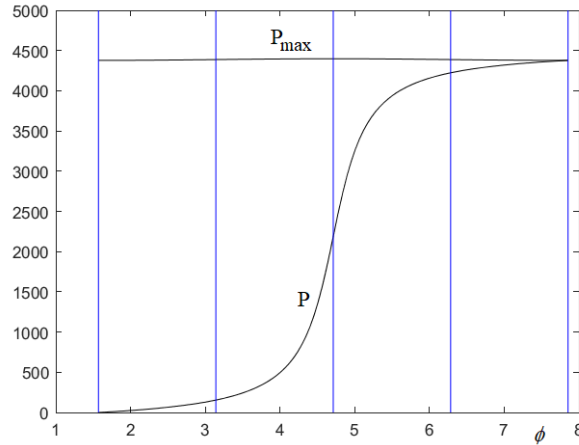


Fig. 6 Power of the engines P as a function of the angle ϕ

$$n = \sqrt{A_c^2 + \cos^2(\theta)} . \tag{41}$$

We consider a circular path centered on the point $[0, 0, 2R]$ on which the airplane starts at the top and goes around it completely, in the positive direction. The distance traveled is $s=R(\phi-\pi/2)$ so that, at the starting point, $s=0$ with $\phi=\pi/2$, and at the final point $s_f=2\pi R$ with $\phi=5\pi/2$. We let the power generated by the engines vary as the following inverse tangent function of s

$$P(s) = \left(\frac{P_M}{2}\right) \left[1 + \frac{\arctan[k(s-R\pi)]}{\arctan[kR\pi]}\right] \tag{42}$$

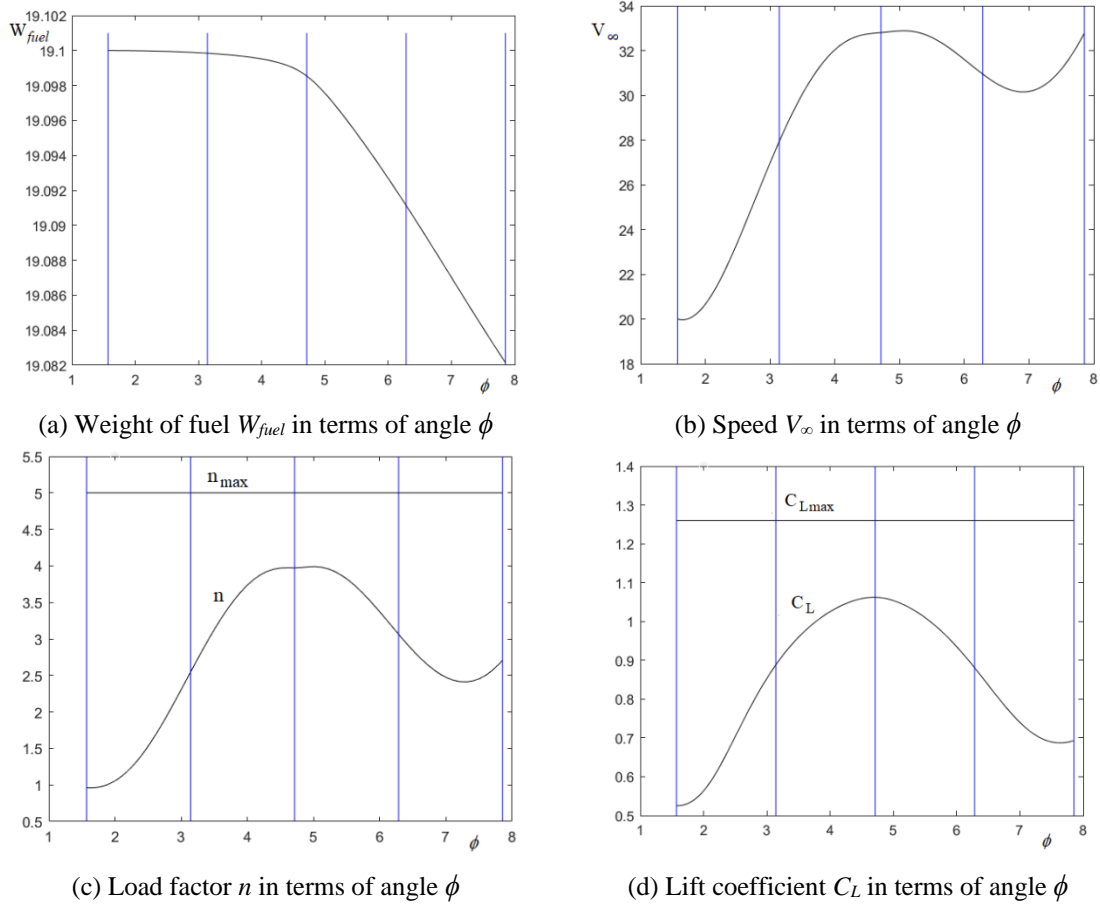
with

$$P_M = P_{max} \frac{\rho_\infty(h_{max})}{\rho_s} \tag{43}$$

in which $h_{max}=R[2+\sin(\theta)]$ is the altitude at the highest point of the path and k is an arbitrarily constant that controls the slope of the arc tangent at the origin. In the present example, we took $k=0.1$. Fig. 6 shows how the power that the engine produces for the Silver Fox-like UAV varies with the distance s traveled around the circle, together with the maximum power P_{max} that it can produce for a circle of radius $R=30$ m. Vertical lines are placed at where ϕ that is a multiple of $\pi/4$. The power $P(s)$ is seen to be very small when the airplane is on the way down and then very large when it is on the way back up.

5.3.1 Silver Fox-like UAV

Consider the Silver Fox-like UAV on a circular path of radius 30 m, inclined at 45° with the horizontal plane. It was shown in Labonté (2016) that there is no constant speed at which this path is flyable. It is however flyable when the power varies according to Eq. (42). We consider a sample flight in which the UAV starts with the initial speed of 20 m/s. It then takes about 6.8 s to fly around the circular path while using 0.018 N of fuel, which is about 2.5 ml. Fig. 7 shows the graphs of the weight of fuel W_{fuel} , the speed V_∞ , the load factor n and the lift coefficient C_L as

Fig. 7 Dynamic parameters of the trajectory in terms of the angle ϕ

functions of the angle ϕ . Vertical lines are placed at each position that corresponds to an angle ϕ multiple of $\pi/2$. As can be seen in these graphs; all the constraints are satisfied.

Our R-K 4 calculations have been done with $dt=0.1$ s. The estimates of the truncation errors, according to Eq. (28), are

- for the amount of fuel used: less than 7.4×10^{-5} N
- for the speed: less than 0.1 m/s
- for the load coefficient: less than 0.022
- for the lift coefficient less than 9.6×10^{-4}

Again, the R-K 4 method can then be considered to yield, for all practical purposes, exact solutions. The average computation time for 10 runs is 0.038 s.

We have tested the flyability of circular trajectories at different angles of inclination. We found that they are all flyable, for some values of the speed, even for very inclined paths. For example, we have checked that a vertical circular path of radius $R=25$ m and initial speed of 17 m/s is flyable. It was shown in Labonté (2016) that there is no constant speed at which the Silver Fox-like UAV can fly on circular trajectory inclined at 15° or more. Thus, clearly, varying the power can ameliorate greatly the flyability of trajectories.

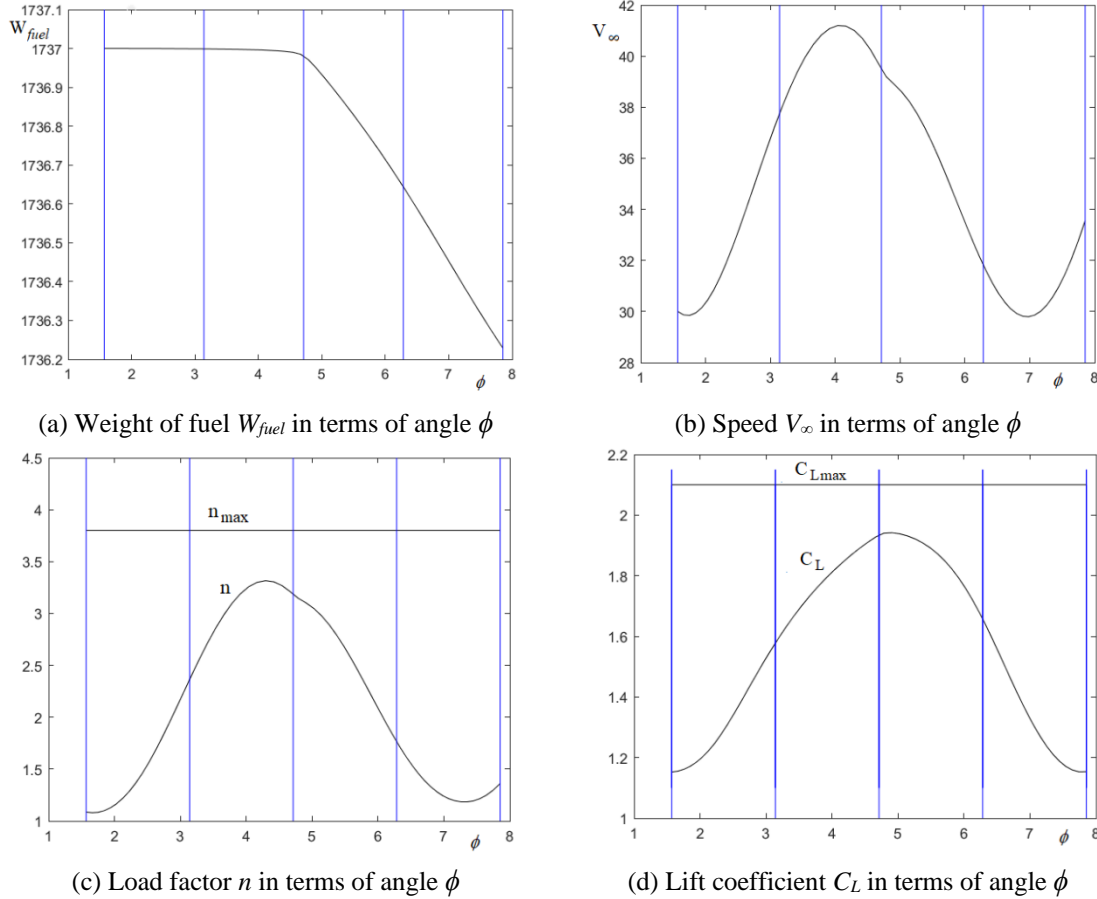


Fig. 8 Dynamic parameters of the trajectory in terms of the angle ϕ

5.3.2 Cessna 182 Skylane

Consider the Cessna on an inclined circular path inclined at 40° , with a radius of 65 m. It was shown in Labonté (2016) that it cannot fly on such a circular path at any constant speed. However, this path becomes flyable by the Cessna when its power varies according to Eq. (42). For example, all the constraints are satisfied when it starts with the initial speed of 30 m/s. It then takes about 12.5 s to fly around the circular path and uses about 0.853 N of fuel, which is about 117.2 ml. The R-K 4 calculations have been done with $dt=0.2$ s. The flight parameters vary much like those of the Silver Fox UAV, shown in Fig. 8.

The estimates of the truncation errors, according to Eq. (28), are

- for the amount of fuel used: less than 2.8×10^{-3} N
- for the speed: less than 0.05 m/s
- for the load coefficient: less than 0.004
- for the lift coefficient less than 2.4×10^{-4}

Again, the R-K 4 method can then be considered to yield, for all practical purposes, exact solutions. The average computation time for 10 runs is 0.046 s.

6. Conclusions

The results presented in this article are quite general and constitute important tools not only for UAV trajectory planning, but also for the analysis of the motion of all fixed-wing propeller driven airplanes. An important contribution of this work is a new relatively simple approach to deal with the equations of motion of the airplane, when its power is specified, so as to determine the value of its dynamical parameters on a trajectory. We believe that this approach is original as we could not find it in any other published material. We show how to solve the equations of motion with the Runge-Kutta method of order 4. Examples are then provided with two very different types of airplanes: a Silver Fox-like small UAV and a common Cessna 182 Skylane. The trajectories considered are a glide on a descending rectilinear path at power off, a climb at full power on a rectilinear path and a circular loop with a power that varies as an arctangent of the angle. The latter example is quite interesting in itself because this type of motion has never been considered before, and it has the particularly interesting property of allowing motion on paths inclined at steep angles. In all the examples considered, the errors done in the numerical solution of the differential equations by the R-K 4 method, are evaluated and shown to be negligible. The calculation times, averaged over ten runs, are given for each example. They are seen to be always below 1 s. We have shown that much more varied trajectories are flyable than those flown at constant speed, as are considered in so many articles on trajectory planning. This fact provides a strong incentive for the enterprise of optimizing the trajectories by controlling the power of the engine.

References

- Aeronautics Learning Laboratory for Science Technology and Research (ALLSTAR) of the Florida International University (2011), Propeller Aircraft Performance and The Bootstrap Approach, <https://web.eng.fiu.edu/allstar/index.htm>.
- Airliners.net (2015), <http://www.airliners.net/aircraft-data/stats.main?id=145>, Santa Monica, CA, USA.
- Ait Saadi, A., Soukane, A., Meraihi, Y., Benmessaoud Gabis, A., Mirjalili, S. and Ramdane-Cherif, A. (2022), "UAV path planning using optimization approaches: A survey", *Arch. Comput. Meth. Eng.*, **29**(6), 4233-4284. <https://doi.org/10.1007/s11831-022-09742-7>.
- Anderson, J.D. and Bowden, M.L. (2005), *Introduction to Flight*, Vol. 582, McGraw-Hill Higher Education, New York.
- Cavcar, M. (2004), "Propeller", School of Civil Aviation, Eskisehir, Turkey.
- Commercial Aviation Safety Team (CAST) (2011), Propeller Operation and Malfunctions Basic Familiarization for Flight Crews, http://www.cast-safety.org/pdf/4_propeller_fundamentals.pdf.
- Cowley, W.L. and Levy, H. (1920), *Aeronautics in Theory and Experiment*, 2nd Edition, Edward Arnold Publisher, London, UK.
- Frazzoli, E., Dahleh, M.A. and Feron, E. (2005), "Maneuver-based motion planning for nonlinear systems with symmetries", *IEEE Trans. Robot.*, **21**(6), 1077-1091. <https://doi.org/10.1109/TRO.2005.852260>.
- Gramajo, G. and Shankar, P. (2017), "An efficient energy constraint based UAV path planning for search and coverage", *Int. J. Aerosp. Eng.*, **2017**, Article ID 8085623. <https://doi.org/10.1155/2017/8085623>.
- Granelli, F. (2007), Carl Goldberg Falcon 56, The Academy of Model Aeronautics' Sport Aviator, the E-Zine for the Newer RC Pilot, December.
- Horizon Hobby (2017), [https://www.horizonhobby.com/product/airplanes/airplane-accessories/airplane-engines-15042--1/gt80-twin-cylinder-\(488-cu-in\)-zene80t](https://www.horizonhobby.com/product/airplanes/airplane-accessories/airplane-engines-15042--1/gt80-twin-cylinder-(488-cu-in)-zene80t). (accessed 04 Sept 2023)
- Kamm, R.W. (2002), "Mixed up about fuel mixtures", *Aircraft Maintenance Technology*, February.
- Labonté, G. (2012), "Formulas for the fuel of climbing propeller driven planes", *Aircraft Eng. Aerosp.*

- Technol.*, **84**(1), 23-36. <https://doi.org/10.1108/00022661211194951>.
- Labonté, G. (2016), “Airplanes at constant speeds on inclined circular trajectories”, *Adv. Aircraft Spacecraft Sci.*, **3**(4), 399-425. <https://doi.org/10.12989/aas.2016.3.4.399>.
- Labonté, G. (2017), “Low thrust inclined circular trajectories for airplanes”, *Adv. Aircraft Spacecraft Sci.*, **4**(3), 237-267. <https://doi.org/10.12989/aas.2017.4.3.237>.
- Labonté, G. (2020), “How airplanes fly at power-off and full-power on rectilinear trajectories”, *Adv. Aircraft Spacecraft Sci.*, **7**(1), 53-78. <https://doi.org/10.12989/aas.2020.7.1.053>.
- Lotkin, M. (1951), “On the accuracy of Runge-Kutta’s method”, *Math. Comput.*, **5**, 128-133.
- Mair, W.A. and Birdsall, D.L. (1992), *Aircraft Performance, Cambridge Aerospace Series 5*, Cambridge University Press, Cambridge, GB.
- McIver, J. (2003), *Cessna Skyhawk II/100, Performance Assessment*, Temporal Images, Melbourne, Australia.
- Military, https://www.militaryfactory.com/aircraft/detail.php?aircraft_id=2003#specifications.
- Poudel, S., Arafat, M.Y. and Moh, S. (2023), “Bio-inspired optimization-based path planning algorithms in unmanned aerial vehicles: A survey”, *Sensor.*, **23**(6), 3051. <https://doi.org/10.3390/s23063051>.
- Roud, O. and Bruckert D. (2006), *Cessna 182 Training Manual*, Red Sky Ventures and Memel CATS, Second Edition 2011, Windhoek, Namibia.
- Stengel, R.F. (2004), *Flight Dynamics*, Princeton University Press, Princeton, New Jersey.
- Varsha, N. and Somashekar, V. (2018), “Conceptual design of high performance unmanned aerial vehicle”, *IOP Conf. Ser.: Mater. Sci. Eng.*, **376**(1), 012056. <https://doi.org/10.1088/1757-899X/376/1/012056>.
- Von Mises, R. (1945), *Theory of Flight*, Dover Publications Inc., New York, NY, USA.

Appendix A: Nomenclature

a =speed of sound in air. At altitude h , $a(h)=\sqrt{\gamma RT(h)}$. At sea level, $a(0)=340.3029$ m/s
 where γ =ratio of the constant pressure specific heat to the constant volume specific heat= $c_p/c_v=1.4$
 for air, R =specific gas constant for air= 287.058 J/(kg K) and $T(h)$ is the temperature of the air.
 AFR=air fuel ratio (about 14.7)

AR=aspect ratio= b^2/S

b =wingspan

c =specific fuel consumption in Newton per Watt-second, that is in m^{-1}

C_D =global drag coefficient for the aircraft= $C_{D0} + \frac{C_L^2}{\pi e AR}$ (Drag polar)

C_{D0} =global drag coefficient at zero lift

C_L =global lift coefficient for the aircraft

D =drag= $\frac{1}{2}\rho_\infty S C_D V_\infty^2$

e =Oswald's efficiency factor

g =gravitational constant= 9.8 m/s²

h =altitude of airplane

h_c =service ceiling

L =lift= $\frac{1}{2}\rho_\infty S C_L V_\infty^2$

P_P =power produced by the engine in Watt: $P_P(h) = P_P(h_0) \frac{r_\infty(h)}{r_\infty(h_0)}$

P_{Pmax} =maximum power that the engines can produce

P_A =power available for the motion= ηP_P in which η =propeller efficiency

P_R =power required for the motion

S =wing area

t =time variable

T =thrust= P/V ;

T_s =temperature at sea level= 288.16 K

$T(h)$ =temperature at altitude $h=T_s-a_1h$ with $a_1=6.5 \times 10^{-3}$

a_1 =absolute value of the slope of the temperature as a function of altitude, below 11 km,

$a_1=6.5 \times 10^{-3}$ K/m

V_∞ =airplane speed with respect to the undisturbed air in front of it

V_{NE} =speed never to be exceeded as specified by the airplane constructor

W =weight of the airplane

W_1 =weight of the empty airplane

W_f =maximum weight of fuel

W_0 =maximum take-off weight (MTOW)

ρ_s =air density at sea level= 1.225 kg/m³

$\rho_\infty(h)$ =density of undisturbed air in front of airplane, at altitude h , $\rho_\infty(h) = \rho_s \left[\frac{T(h)}{T_s} \right]^{4.2433}$

Appendix B: Reference airplanes

B.1 Silver Fox-like UAV

The Silver Fox UAV is presently produced by Raytheon. Some of its specifications can be found at Military Factory Raytheon Silver Fox and Manufacturers (2016). The power produced at sea level $P_{\max}(0)$ for the Silver Fox is only about 370 W, which only allows it to climb at low angles. Meanwhile, it is common for Radio Controlled (RC) airplanes to climb at very steep angles (See for example Granelli 2007). Thus, upon taking advantage of motors that have been developed in this domain, a Silver Fox-like airplane could be endowed with much more power in order to improve considerably its manoeuvre envelope. One such motor is the Zenoah GT-80 Twin Cylinder 80cc (ZENE80T). It weighs 34 N and outputs 4045 W at 7500 rpm. (Horizon Hobby 2017). We shall consider a Silver Fox-like UAV with such a motor.

Table 1 shows the values of the following parameters W_1 =the weight of the empty airplane, W_0 =the maximum take-off weight, W_F =the maximum weight of fuel, b =the wingspan, S =the wing area, e =Oswald's efficiency factor, $C_{L\max}$ =the maximum global lift coefficient, C_{D0} =the global drag coefficient at zero lift, n_{\max} and n_{\min} are respectively the maximum and minimum value of the load factor, P_{\max} =maximum breaking power at sea level, RPM=number of revolution per minute, Diameter=diameter of the propeller, η_{\max} =maximum value of the propeller efficiency, h_c =service ceiling.

Table 1 Characteristic parameters of the Silver Fox-Like airplane

$W_1=100.0$ N	$W_0=148.0$ N	$W_F=19.1$ N
$b=2.4$ m	$S=0.768$ m ²	$e=0.8$
$C_{L\max}=1.26$	$C_{D0}=0.0251$	$n_{\max}=5.0, n_{\min}=-2.0$
$P_{\max}=4.413$ kW	RPM=7500	$c=7.4475 \times 10^{-7}$
Fixed pitch propeller	Diameter=0.56 m	$\eta_{\max}=0.77$
$h_c=3700$ m		

B.2 Cessna 182 Skylane

The characteristic parameters for the Cessna 182 can be found in Airliners.net (2015), Roud and Bruckert (2006) and McIver (2003). Some of the parameters, which were not readily available, were estimated from those of the very similar Cessna 172.

Table 2 Characteristic parameters of the Cessna 182

$W_1=7,562$ N	$W_0=11,121$ N	$W_F=1,737$ N
$b=11.02$ m	$S=16.1653$ m ²	$e=0.75$
$C_{L\max}=2.10$	$C_{D0}=0.029$	$n_{\max}=3.8, n_{\min}=-1.52$
$P_{\max}=171.511$ kW	RPM=2,600	$c=7.4475 \times 10^{-7}$
Const. speed propeller	Diameter=2.08 m	$\eta_{\max}=0.80$
$h_c=5500$ m		

B.3 Propeller efficiency

The thrust of the Silver Fox is provided by a reciprocating engine with fixed pitch. We recall that the efficiency of the propeller is a function of the advance ratio J , defined as:

$$J = \frac{V_\infty}{ND}$$

in which N is its number of revolutions per second and D is its diameter. Thus the maximum power available P_{Amax} will depend on the speed, according to the equation:

$$P_{Amax} = \eta(J)P_{max}$$

The dependence of η on J for a constant speed propeller has the general features shown in Fig. 9(a). This curve approximates that given in Cavcar (2004) by the following quadratic expressions:

$$\eta(J) = \begin{cases} \left[\frac{0.663}{0.640} \right] [J - 0.8]^2 + 0.8 & \forall J \leq 0.8 \\ 0.8 & \forall J > 0.8 \end{cases}$$

The dependence of η on J for a fixed pitch propeller has the general features shown in Fig. 9(b). This curve approximates that given in the Aeronautics Learning Laboratory for Science Technology and Research (ALLSTAR) of the Florida International University (2011) by the following quadratic expressions:

$$\eta(J) = \begin{cases} -\left[\frac{0.83}{0.49} \right] [J - 0.70]^2 + 0.83 & \forall J \leq 0.7 \\ -\left[\frac{0.83}{0.06} \right] [J - 0.70]^2 + 0.83 & \forall J > 0.7 \end{cases}$$

Note that the propeller efficiency of this fixed pitch propellers goes to 0 at $V_\infty=66.1$ m/s and becomes negative after that. Although a negative propeller efficiency might be desirable to slow down the airplane when it descends, it is not recommended to let this happens. When this happens, the propeller drives the engine and damage to the engine may result [see for example the Commercial Aviation Safety Team document (2011)]. We shall therefore not allow speeds larger than that value.

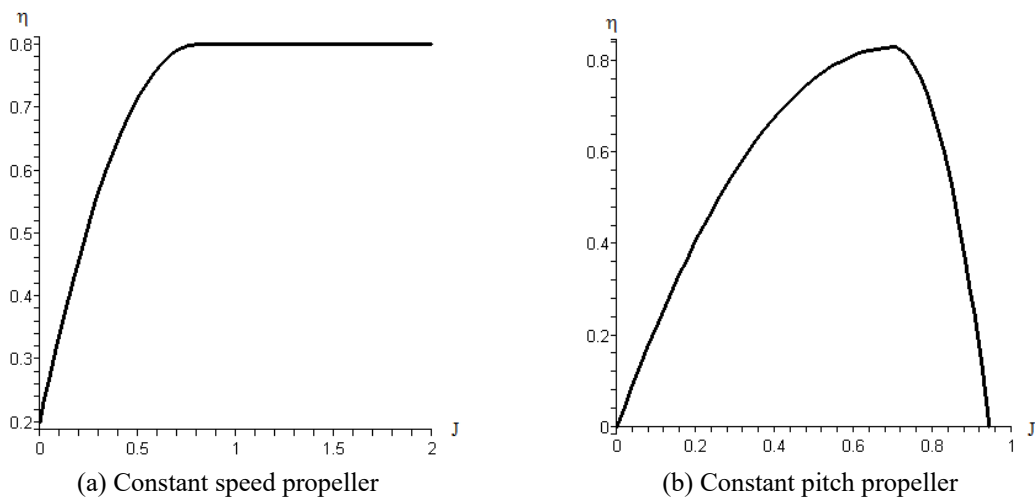


Fig. 9 Typical efficiency factor η as a function of the advance ratio J